RESEARCH ARTICLE OPEN ACCESS

Design of Digital Autopilot for Lateral Motion Control of an Aircraft Based on l_1-Optimization Approach

Leonid S. Zhiteckii, Valerii N. Azarskov, Andriy Yu. Pilchevsky, Klavdia Yu. Solovchuk

ABSTRACT
The optimal digital autopilot needed to control of the roll for an aircraft in the presence of an arbitrary unmeasured disturbances is addressed in this paper. Such autopilot has to achieve a desired lateral motion control of this aircraft via minimizing the upper bound on the absolute value of the difference between the given and true roll angles. It is ensured by means of the two digital controllers. The inner controller is designed as the discrete-time PI controller in order to stabilize a given roll rate. This variable is formed by the external P controller. The necessary and sufficient conditions under which the two-circuit feedback discrete-time control system will be stable are derived. To optimize this control system, the controller parameters are derived utilizing the so-called l_1-optimization approach advanced in modern control theory. A numerical example demonstrating the l_1-optimization technique and results of some simulation experiments are presented to illustrate the performance of the l_1-optimal controller. The robustness properties of this controller are established.
Index Terms-Aircraft, Lateral Dynamics, Digital Control System, Discrete Time, Stability, l_1-Optimization, Random Search Algorithm, Robustness.

I. INTRODUCTION

The problem of efficiently controlling the motion of an aircraft in a non-stationary environment capable to ensure its high performance index is important enough from the practical point of view and remains actual up to now [1], [2]. To solve this problem, different approaches based on achievements of the modern control theory, including adaptive and robust control, neural networks, etc., have been reported by many researches (see, for example, [3] – [9]). Recently, new results in this research direction have been presented, in particular, in [10]. Unfortunately, most of these works dealt with an ideal case when there are no external persistently exciting disturbances. Nevertheless, they are always present in reality. To implement approaches advanced in modern control theory, digital technique is appropriate. Point is that, by the end of the twentieth century, digital control has become a highly developed technology in control applications [11], [12]. Digital control systems have some features associated with sampling [12], [13]. Namely, it leads to arising the discrete-time system description. It turns out that accurate discrete-time models can be derived for sampled continuous-time systems under digital control [14]. One of the efficient methods devised in the modern control theory for rejecting any unmeasured disturbance is based on the so-called l_1-optimization concept [15] – [17] applicable to discrete-time control systems. This concept has been utilized in [18] to design the digital lateral autopilot for an UAV capable to cope with a gust.In order to implement the l_1-optimization of any digital controller, the information with respect to the dynamics model of a plant to be controlled including its structure and parameters is required. In practice, however, it may not be available in full detail. In this real situation, the following question naturally arises: is the l_1-optimal PI controller designed via the use of a priori knowledge of the so-called nominal lateral dynamics model robust? This paper extends the approach which we have first reported among other authors in [18] to deal with a digital autopilot for the lateral motion control. Its aim is to synthesize a digital autopilot which is able to maintain a given roll orientation of an aircraft with a desired accuracy and to reject an arbitrary external disturbance (in particular, the gust). Again, this controller needs to be robust with respect to parametric and nonparametric uncertainties. As in traditional continuous-time (analogue) control systems [5], the digital control system is designed as the two-circuit closed-loop system having the inner feedback loop and the external feedback loop. The distinguishing feature of the digital autopilot is that it is designed as the so-called l_1-optimal controller containing the discrete-time PI and P controllers.

The novel contribution of this paper includes the following:

1. The l_1-optimal PI and P controller parameters of the digital autopilot are calculated simultaneously (in contrast with [18]).
2. The aileron servo dynamics is taken into account to derive the stability condition for l_1-optimizing the controller parameters.

3. Random search algorithm is used to find the three optimal values of the autopilot parameters.
4. Robustness properties of the l_1-optimal autopilot are established.

The rest of the paper is organized as follows. In Section II, the problems of the designing the l_1-optimal autopilot is stated. Section contains the main results of this work and deals with the synthesis of l_1-optimal controller needed to achieve the perfect performance of the lateral motion of an aircraft. In Section IV, a numerical example is given. In Section V, the robustness properties of l_1-optimal autopilot are established and results of some simulation experiments are presented. Section VI concludes this paper.

II. PROBLEM FORMULATION

A. Basic Assumptions

Let $\dot{\gamma}(t)$ and $\xi(t)$ denote the roll rate angle and the aileron deflection of an aircraft, respectively, at a time t. According to [19, chap. 3] its lateral dynamics equation derived from the linearized lateral equation of the aircraft motion can be described by the continuous-time transfer function

$$W_{\xi}(s) = \frac{1}{s}\tilde{W}_{\xi}(s) = \frac{K_{\xi}}{s(T_{\xi}s+1)}, \qquad (1)$$

where K_{ξ} and T_{ξ} are the aerodynamic derivatives (more specifically, T_{ξ} is the damping derivative in the roll channel and K_{ξ} is the roll moment).

B. Control Objective

Denote by $\gamma^0(t)$ the desired roll orientation at the time t. It is assumed that $\gamma^0(t)$ is a continuous upper bounded function of t. This means that there exists a constant $C_{\dot{\gamma}}$ such that

$$|\dot{\gamma}^0(t)| \le C_{\dot{\gamma}} < \infty. \qquad (4)$$

Defining now the output error

$$e(t) = \gamma^0(t) - \gamma(t), \qquad (5)$$

introduce the performance index of the control system to be designed as

$$J := \lim_{t\to\infty} \sup |\gamma^0(t) - \gamma(t)|. \qquad (6)$$

The problem to be stated is formulated as follows. Devise a digital controller which is able to minimize J given by (6) assuming that the variables $\gamma(t)$ and $\dot{\gamma}(t)$ can be measured and the constraints of the forms (3) and (4) take place. Hence, the aim of the controller design may be written as the requirement

$$\lim_{t\to\infty} \sup |e(t)| \to \inf_{\{u(t)\}}, \qquad (7)$$

where (5) has been utilized. The controller satisfying (7) is called optimal.

$u(t)$ using the so-called zero-order hold (ZOH) [11], [13]. This makes it possible to represent the control input, $u(t)$ as follows:

As in [19, chap. 4], it is assumed that continuous-time transfer function describing the aileron servo dynamics is

$$W_S(s) = \frac{K_S}{T_S s + 1}, \qquad (2)$$

where K_S and T_S are its gain and time constant, respectively.

Let $d(t)$ be an external signal (in particular, a gust) disturbing the angular velocity $\dot{\gamma}$. This signal plays a role of some unmeasurable arbitrary disturbance. Without loss of generality, it is assumed that it has to be upper bounded in modulus. This implies that

$$|\dot{d}(t)| \le C_{\dot{d}} < \infty. \qquad (3)$$

The question that we also need to answer in this paper is as follows. Can this l_1-optimal controller be robust?

III. DIGITAL LATERAL AUTOPILOT DESIGN

A. Control Strategy

To implement the controller design concept proposed in this paper, two feedback loops similar to that in [18], [19] are incorporated in the autopilot system, as shown in Fig. 1. But, in contrast with [19], they are designed as the discrete-time closed-loop control circuits using two separate controllers. To this end, two samplers are incorporated in the feedback loops; see Fig. 1. These samplers are required in order to convert analogue signals $\dot{\gamma}(t)$ and $\gamma(t)$ in digital form at each *n*th time instant $t = nT_0$ $(n = 0, 1, 2, \dots)$ to producing the discrete-time signals $\dot{\gamma}(nT_0)$ and $\gamma(nT_0)$, respectively, with the sampling period T_0. On the other hand, the signal $u(nT_0)$ formed by digital controller at the same time instant converts to analogue form

$$u(t) = u(nT_0) \quad \text{for} \quad nT_0 \le t < (n+1)T_0.$$

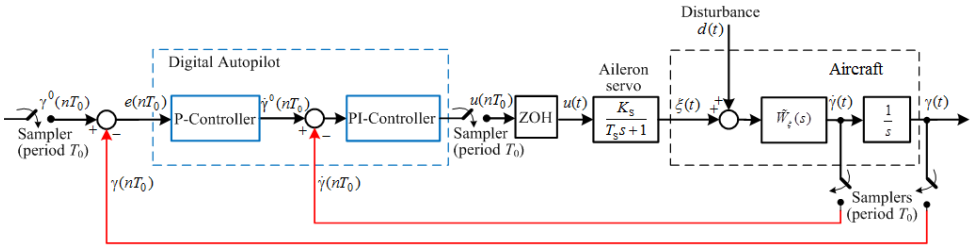

Fig. 1. Structure of digital autopilot system

The aim of the inner control loop exploiting the discrete-time PI control is to stabilize the roll rate $\dot{\gamma}(nT_0)$ at a given value, $\dot{\gamma}^0(nT_0)$, which is the output of the external control loop, as shown in Fig. 1. The feedback control law of this digital controller is

$$u(nT_0) = k_p^{in} e_{\dot{\gamma}}(nT_0) + k_I^{in} \sum_{i=0}^{n} e_{\dot{\gamma}}(iT_0) \qquad (8)$$

where $e_{\dot{\gamma}}(nT_0)$ is the deflection of the true angular velocity, $\dot{\gamma}(nT_0)$, from a given angular velocity, $\dot{\gamma}^0(nT_0)$, at the time instant $t = nT_0$ given by

$$e_{\dot{\gamma}}(nT_0) = \dot{\gamma}^0(nT_0) - \dot{\gamma}(nT_0),$$

and k_p^{in} and k_I^{in} represent the PI controller parameters.

The sampled-data transfer function derived from (8) is determined as follows:

$$C^{in}(z) := \frac{U(z)}{E_{\dot{\gamma}}(z)} = k_p^{in} + \frac{k_I^{in} z}{z-1},$$

Where $U(z) := Z\{u(nT_0)\}$ and $E_{\dot{\gamma}}(z) := Z\{e_{\dot{\gamma}}(nT_0)\}$ are the *Z*-transforms of the sequences $\{u(nT_0)\}$ and $\{e_{\dot{\gamma}}(nT_0)\}$, respectively.

The external feedback loop which contains the usual P controller is used to stabilize the roll angle, $\gamma(nT_0)$, around the desired value, $\gamma^0(nT_0)$. Its control law is defined by

$$\dot{\gamma}^0(nT_0) = k_p^{ex} e_{\gamma}(nT_0) \qquad (9)$$

together with the discrete-time output error

$$e(nT_0) = \gamma^0(nT_0) - \gamma(nT_0). \qquad (10)$$

Then the sampled-data transfer function corresponding to (9), (10) will be defined as

$$C^{ex}(z) = k_p^{ex}. \qquad (11)$$

In order to choose the optimal parameters of both digital controllers, the so-called l_1-optimization approach is utilized.

B. Background on l_1-Optimization Concept

Before going to the l_1-optimization concept consider at first a pure discrete-time system depicted in Fig. 2. Let its dynamics be described by a sampled-data transfer function $H(z)$ which causes

$$Y(z) = H(z)X(z) \qquad (12)$$

with corresponding $X(z) = Z\{x_n\}$ and $Y(z) = Z\{y_n\}$.

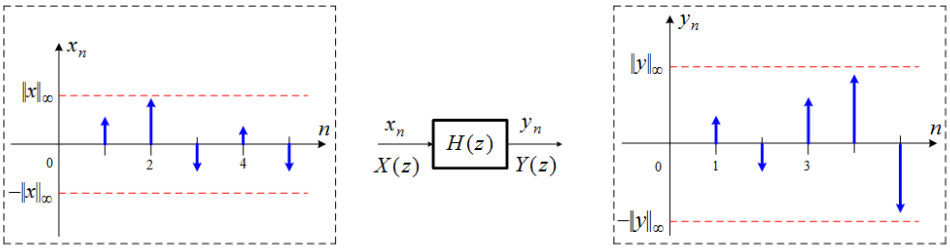

Fig. 2. Schematic representation of a pure discrete-time system

If initial conditions are zero, then (12) yields [18]

$$y_n = \sum_{i=0}^{n} h_i x_{n-i} \qquad (13)$$

Suppose that $\{x_n\}$ is upper bounded implying

$$\| x \|_\infty := \sup_{0 \le n < \infty} | x_n | < \infty, \qquad (14)$$

where $\| \cdot \|_\infty$ denotes the so-called l_∞-norm of the corresponding sequence; see [20, item 1.3.1].
With zero initial conditions, due to (13) together with (14) one can write the inequality

$$\sup_{\{x_n\} \in \ell_\infty} | y_n | \le \| x \|_\infty \sum_{i=0}^{n} | h_i | \qquad (15)$$

in which the notation l_∞ of the set of all bounded sequences taken from [20] is introduced.
It is known that if $H(z)$ is an asymptotically stable discrete-time transfer function, then (15) produces

$$\| y \|_\infty \le \| H \|_1 \| x \|_\infty < \infty, \qquad (16)$$

where $\| y \|_\infty := \sup_{0 \le n < \infty} | y_n |$, and $\| H \|_1$ represents the so-called l_1-norm of $H(z)$ defined as [20, item 1.3.3]

$$\| H \|_1 := \sum_{n=0}^{\infty} | h_n |. \qquad (17)$$

In the expression (17), h_n represents the impulse response of H at *n*th time instant determined as the inverse *Z*-transform of $H(z)$:

$$h_n = Z^{-1}\{H(z)\}.$$

(More exactly, $\| H \|_1$ is indeed the l_1-norm of $\{h_n\}$ having the property that

$$h_0 + h_1 + h_2 + \ldots$$

is the absolutely convergent series, i.e., $\sum_{n=0}^{\infty} | h_n | < \infty$ but not of $H(z)$.)
According to the definition (17), the variable $\| H \|_1$ is evaluated by summing the absolute values of h_is from $i = 0$ to $i = n$ and by increasing the number *n*. Suitable estimate of $\| H \|_1$ is obtained if *n* is sufficiently large number.
In general, for any initial x_0, x_{-1}, x_{-2},..., instead of (16), the following inequality can be shown to be valid:

$$\limsup_{n \to \infty} | y_n | \le \| H \|_1 \| x \|_\infty < \infty.$$

Now, to clarify the l_1-optimization approach, the typical digital feedback control system subjected to external unmeasurable continuous-time disturbance, $d(t)$, is depicted in Fig. 3. This system contains continuous plant described by some transfer function $P(s) = P'(s)P''(s)$ and a digital controller whose sampled-data transfer function is $C(z)$.

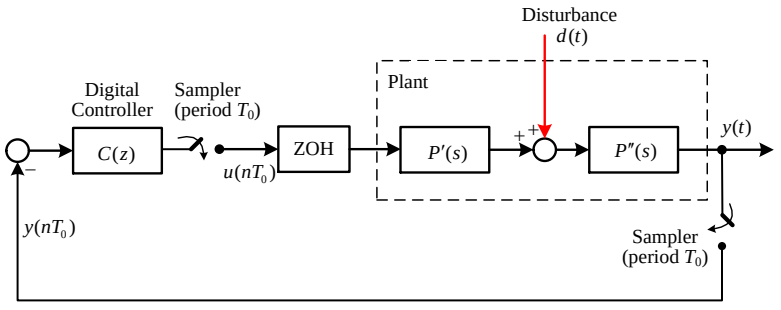

(a)

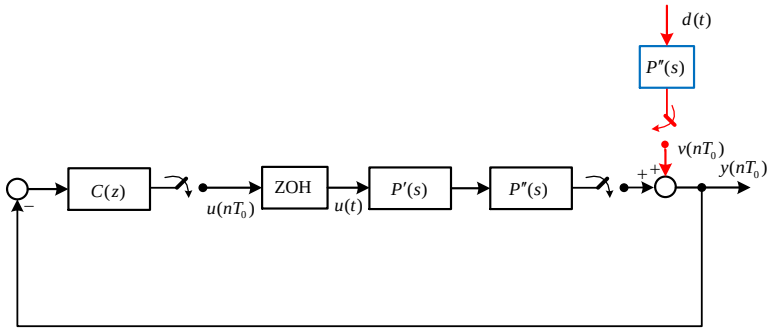

(b)

Fig. 3. Basic feedback loop configuration of digital control system in the presence of a continuous-time disturbance

According to [22, subsect. 10.5], after the inspection of Fig. 3(a) it can be written

$$Y(z) = H(z)P''D(z), \quad (18)$$

where

$$H(z) = \frac{1}{1 + C(z)P'P''(z)} \quad (19)$$

in which

$$P'P''(z) = (1 - z^{-1})Z\left\{L^{-1}\left\{\frac{P'(s)P''(s)}{s}\right\}_{t=nT_0}\right\}$$

(see [14, Lemma 3.5]). $P''D(z)$ denotes the *Z*-transform of the sequence $\{v(nT_0)\}$ formed via sampling the continuous-time signal

$$v(t) = L^{-1}\{P''(s)D(s)\}$$

resulting in

$$V(z) := P''D(z) = Z\left\{L^{-1}\{P''(s)D(s)\}_{t=nT_0}\right\}. \quad (20)$$

The equations (18) to (20) make it possible to move from the initial block diagram of closed-loop discrete-time control system with a continuous-time signal shown in Fig. 3(a) to its equivalent block diagram presented in Fig. 3(b). This fact will be used later for l_1-optimizing the control system whose block diagram has been depicted in Fig. 1.

It can easily be clarified that if either $C(z)$ has the one pole at $z = 1$ or $P''(s)$ has the one pole at $s = 0$ then $H(z)$ will be

$$H(z) = (z-1)H'(z) \quad (21)$$

that, by virtue of (18) together with (20), gives

$$Y(z) = H'(z)[(z-1)V(z)]. \quad (22)$$

If the part P'' of the plant is simply stable (the asymptotic stability is not necessary) and the assumption (3) is satisfied then the variable $\Delta v_n := v_{n+1} - v_n$ will be upper bounded in modulus implying $\|\Delta v\|_\infty := \sup_{0 \le n < \infty} |v_n| < \infty$.

Since $\Delta v_n = Z^{-1}\{(z-1)P''D(z)\}$, the ultimate inequality

$$\limsup_{n\to\infty} |y_n| \le \|H'\|_1 \|\Delta v\|_\infty < \infty. \quad (23)$$

follows directly from (22) for this case.

Now, assuming the plant parameters to be fixed, one can see from (19), (21) that $\|H'\|_1 = \|H'(k_C)\|_1$ depends only on a vector k_C of controller parameters setting $C(z) = C(z, k_C)$. (Note that $\|\Delta v\|_\infty$ is independent of k_C). Thus, (23) can be rewritten as

$$\limsup_{n\to\infty} |y_n| \le \|H'(k_C)\|_1 \|\Delta v\|_\infty < \infty \quad (24)$$

It is clear that $\|H'(k_C)\|_1$ needs to be minimized in k_C to guarantee the minimum of the right side of (24). Namely, l_1-optimization reduces to the problem

$$\|H'(k_C)\|_1 \to \min_{k_C}. \quad (25)$$

C. Stability Analysis.

Inspecting Fig. 1 and recalling the notations (1) and (2), one gets the discrete-time transfer function of inner feedback loop from $\dot\gamma^0$ to $\dot\gamma$ as

$$H^{in}(z) = \frac{C^{in}(z)W_S W_\xi(z)}{1 + C^{in}(z)W_S W_\xi(z)}, \quad (26)$$

where

$$W_S W_\xi(z) = (1 - z^{-1})Z\{L^{-1}\{W_S(s)W_\xi(s)\}_{t=nT_0}\}$$

[21]. Then, using these notations, the expression (26) gives

$$H^{in}(z) = \frac{a_1 z^2 + a_2 z + a_3}{z^3 + b_1 z^2 + b_2 z + b_3}, \quad (27)$$

where

$$\left.\begin{aligned} a_1 &= (k_P^{in} + k_I^{in})c_1, \\ a_2 &= -k_P^{in}c_1 + k_P^{in}c_2 + k_I^{in}c_2, \\ a_3 &= -k_P^{in}c_2, \\ b_1 &= d_1 - 1 + k_P^{in}c_1 + k_I^{in}c_1, \\ b_2 &= d_2 - d_1 - k_P^{in}c_1 + k_P^{in}c_2 + k_I^{in}c_2, \\ b_3 &= -k_P^{in}c_2 - d_2 \end{aligned}\right\} \quad (28)$$

are the coefficients depending on

$$\left.\begin{aligned} c_1 &= [-K_S K_\xi T_S + K_S K_\xi T_S e^{-T_0/T_S} + K_S K_\xi T_\xi - K_S K_\xi T_\xi e^{-T_0/T_\xi}]/(T_\xi - T_S), \\ c_2 &= [-K_S K_\xi T_S e^{-T_0(T_S+T_\xi)/T_S T_\xi} + K_S K_\xi T_S e^{-T_0/T_S} \\ &\quad + [K_S K_\xi T_\xi e^{-T_0(T_S+T_\xi)/T_S T_\xi} - K_S K_\xi T_\xi e^{-T_0/T_\xi}]/(T_\xi - T_S) \\ d_1 &= -e^{-T_0/T_\xi} - e^{-T_0/T_S}, \\ d_2 &= e^{-T_0(T_S+T_\xi)/T_S T_\xi}. \end{aligned}\right\} \quad (29)$$

By applying the stability results with respect to the three-order control system which can be found in [22, subsect. 1.12] to the denominator of $H^{in}(z)$ in (27) we derive the conditions guaranteeing the asymptotic stability of inner closed loop in the form

$$\left.\begin{aligned} &\beta_j > 0, \quad j = 0, 1, 2, 3, \\ &\beta_1\beta_2 - \beta_0\beta_3 > 0 \end{aligned}\right\} \tag{30}$$

with

$$\left.\begin{aligned} \beta_0 &= 1 + b_1 + b_2 + b_3, \\ \beta_1 &= 3(1 - b_3) + b_1 - b_2, \\ \beta_2 &= 3(1 + b_3) - b_1 - b_2, \\ \beta_3 &= 1 - b_1 + b_2 - b_3. \end{aligned}\right\} \tag{31}$$

It turns out that the set Ω^{in} of pairs (k_P^{in}, k_I^{in}) under which the inner loop will be stable is bounded. This fact follows from (30) together with (28), (29) and (31).

In order to study the stability of the external closed loop, we again inspect Fig. 1 to obtain the discrete-time transfer function of the corresponding open loop as

$$G(z) = k_P^{ex} G'(z),$$

where

$$G'(z) = \frac{W_S W_\xi W_0(z)}{1 + C^{in}(z) W_S W_\xi(z)}.$$

Applying the frequency stability criterion taken from [20] we establish that the necessary and sufficient condition under which the closed loop will be stable is given by

$$0 < k_P^{ex} < -m, \tag{32}$$

where

$$m = \min\{\mathrm{Re}\, G(e^{j\omega}) : \mathrm{Im}\, G(e^{j\omega}) = 0\}. \tag{33}$$

According to (32), (33), the set Ω^{ex} of k_P^{ex}s guaranteeing the stability of the external loop is bounded.

D. l_1-Optimization Algorithm

It can be finally established that if T_0 is sufficiently small then

$$\limsup_{n\to\infty} |e_\gamma(nT_0)| \le \|H^{ex}(k_C)\|_1 \|v^{ex}\|_\infty + O(\|\Delta v\|_\infty) < \infty, \tag{34}$$

where

$$H^{ex}(z, k_C) = \frac{1}{1 + C^{in}(z) W_S W_\xi(z) + C^{in}(z) C^{ex}(z) + W_S W_\xi W_0(z)}$$

depends on the vector $k_C = [k_P^{in}, k_I^{in}, k_P^{ex}]^T$ of the controller parameters. (Due to space limitation, details are omitted).

Since Ω^{in} and Ω^{ex} are both bounded, it is possible to utilize the well-known Weierstrass theorem [23, chap. 1, sect 3] to solve the l_1-optimization problem (25). By virtue of this theorem, there exists some

$$k_C^* = \arg \min_{k_C \in \Omega^{in} \times \Omega^{ex}} \|H^{ex}(k_C)\|_1. \tag{35}$$

minimizing the l_1-norm of $H^{ex}(k_C)$ in k_C.

Taking (34) into account, we see that the choice of k_C^* in accordance with (35) solves the l_1-optimization problem formulated as the requirement (6) if only T_0 is small enough. Unfortunately, the l_1-norm of $H^{ex}(k_C)$ is non-differentiable function with respect to the components k_P^{in}, k_I^{in}, k_P^{ex} of k_C. Therefore, the random search technique taken from [23, chap. 6, item 4] is proposed to find the optimal parameter vector k_C^* defined in (35).

The l_1-optimization algorithm employing the random search is as follows:

Step #1: Setting $k = 0$ choose an arbitrary $\hat{k}_C^0 \in \Omega$, where $\Omega = \Omega^{in} \times \Omega^{ex}$ is the De Cartesian product.

Step #2: Compute a trial point $\hat{k}_C^{k+} \in \Omega$, according to the rule

$$\hat{k}_C^{k+} = \hat{k}_C^k + r^k,$$

where r^k is a realization of a suitably distributed random vector.

Step #3: If $\|H(\hat{k}_C^{k+})\|_1 < \|H(\hat{k}_C^k)\|_1$ then $\hat{k}_C^{k+1} = \hat{k}_C^{k+}$, else $\hat{k}_C^{k+1} = \hat{k}_C^k$,

Step #4: Increment *k* by one and go to Step #2.

IV. A NUMERICAL EXAMPLE

Let the nominal (approximate) transfer function $\tilde{W}_\xi(s)$ in (1) be

$$\tilde{W}_\xi(s) = \frac{10.84}{0.4926\, s + 1}$$

that corresponds to the following parameters of an aircraft: $K_\xi = 10.84$ and $T_\xi = 0.4926\,\mathrm{s}$ (as in [19, formula (3.62)]). According to [19, sect. 4.2], the transfer function of aileron servo is given by

$$W_S(s) = \frac{10}{s + 10}$$

that corresponds to $K_S = 1$, $T_S = 0.1\,\mathrm{s}$ in (2).

Choose the sampling period equal to $T_0 = 0.01\,\mathrm{s}$.

By formulas (29), we first calculate $c_1 = 0.0106$, $c_2 = 0.0102$, $d_1 = -1.8847$, $d_2 = 0.8867$.

Next, by using the values of these coefficients, we specify the stability region Ω^{in} of the inner closed loop depicted in Fig. 4. Further exploiting the inequalities (30) together with (31), we are capable to design the three-dimensional stability region

$\Omega = \Omega^{in} \times \Omega^{ex}$ as shown in Fig. 5. Note that $\Omega \subset \Omega_0$, where Ω_0 is an outer parallelepiped .

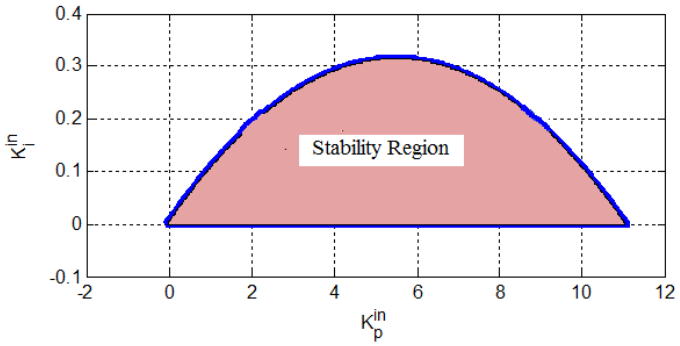

Fig. 4. Stability region of the inner circuit under the conditions of the numerical example

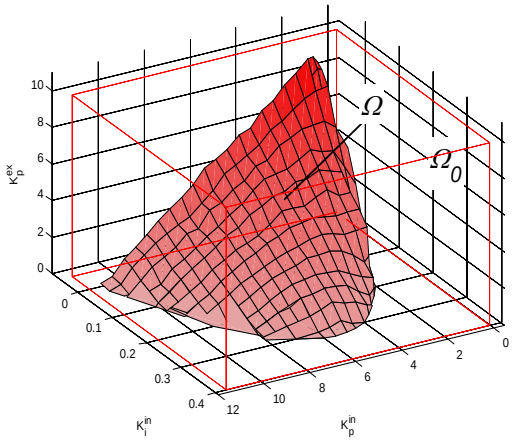

Fig. 5. Stability region of the control system under the conditions of the numerical example

Fig. 6 is presented to demonstrate how the random search process goes step by step utilizing the algorithm described in Section III (D). It shows how the vector sequence $\{k_C^k\}$ generated by this algorithm converges to a $k_C^* \approx [k_P^{in*}, k_I^{in*}, k_P^{ex*}]^T$ equal approximately to $k_C^* = [4,\ 0.1,\ 3.9]^T$.

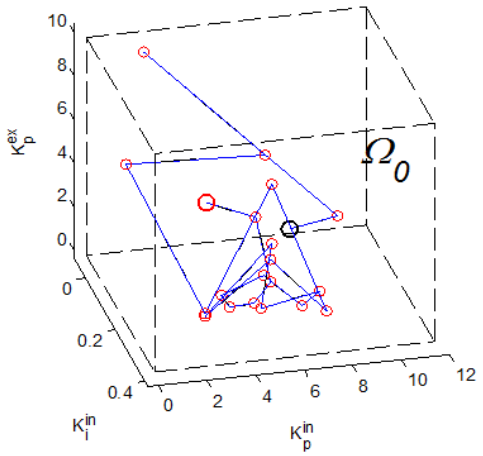

Fig. 6. Trajectory of random vector sequence $\{k_C\}$ from initial k_C^0 (black point) to final $k_C^{21} \approx k_C^*$ (red point) within the stability region of Fig. 5

V. ROBUSTNESS EVALUATION AND A SIMULATION

To study the robustness properties of this l_1-optimal controller under the parametric uncertainty, we assumed that the parameters K_ξ and T_ξ may vary within the following ranges: $\underline{K}_\xi \le K_\xi \le \overline{K}_\xi$ and $\underline{T}_\xi \le T_\xi \le \overline{T}_\xi$ with $\underline{K}_\xi = 8.672$, $\overline{K}_\xi = 12.47$ ($\underline{K}_\xi = 0.8K_\xi$, $\overline{K}_\xi = 1.15K_\xi$) and $\underline{T}_\xi = 0.468$ s, $\overline{T}_\xi = 0.591$ s ($\underline{T}_\xi = 0.95T_\xi$, $\overline{T}_\xi = 1.2T_\xi$), respectively. The parametric uncertainty region corresponding to these ranges defined as $\Xi := [\underline{K}_\xi, \overline{K}_\xi] \times [\underline{T}_\xi, \overline{T}_\xi]$ is depicted in Fig. 7.

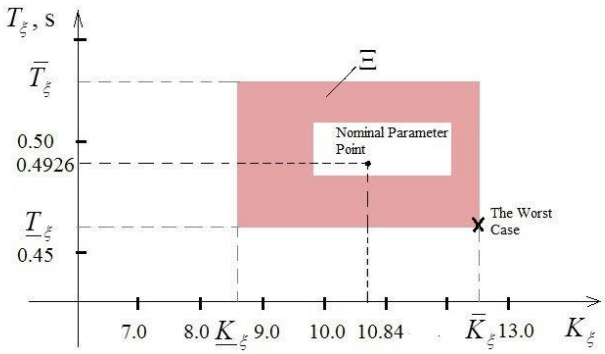

Fig. 7. Parameter uncertainty region

To evaluate the performance index of the control system containing the l_1-optimal controller without and with uncertainties, two simulation experiments were conducted. In these experiments, variable $d(t)$ similar to the wind gust was simulated as Dryden Wind Turbulence Model. It turned out that if the parametric uncertainty is present then the worst case (in the sense of robust stability) is: $K_\xi = \overline{K}_\xi$, $T_\xi = \underline{T}_\xi$ (see Fig. 7). Simulation results corresponding to the absence and the presence of this uncertainty are presented in Fig. 8.

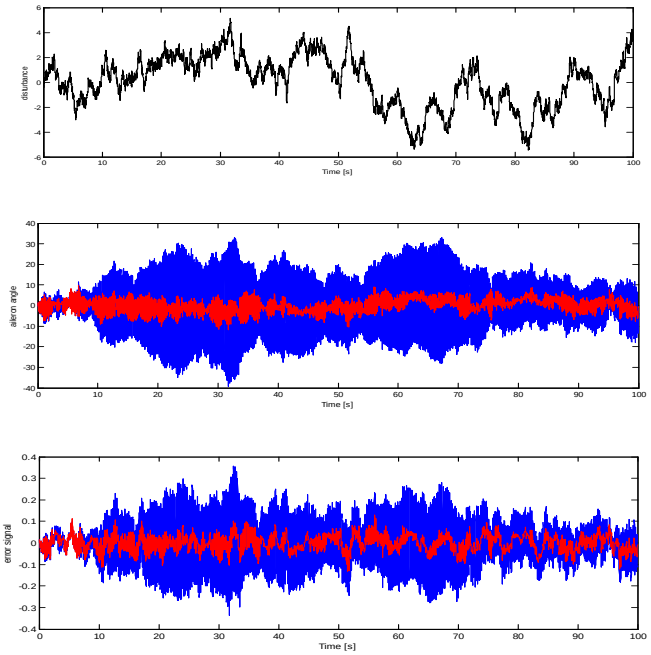

Fig. 8. Behavior of l_1-optimal lateral autopilot without (red color) and with (blue color) parametric uncertainty for the worst case

To study the robustness properties of the l_1-optimal controller under nonparametric uncertainty,

$$\tilde{W}_{\xi}(s) = \frac{0.171s(s+18.75)(s+0.15)}{(s^2+0.380s+1.813)(s+2.09)(s-0.004)}$$

taken from [19, formula 3.51) was set (instead of the previous $\tilde{W}_{\xi}(s)$). Simulation results corresponding to this case are presented in Fig. 9.

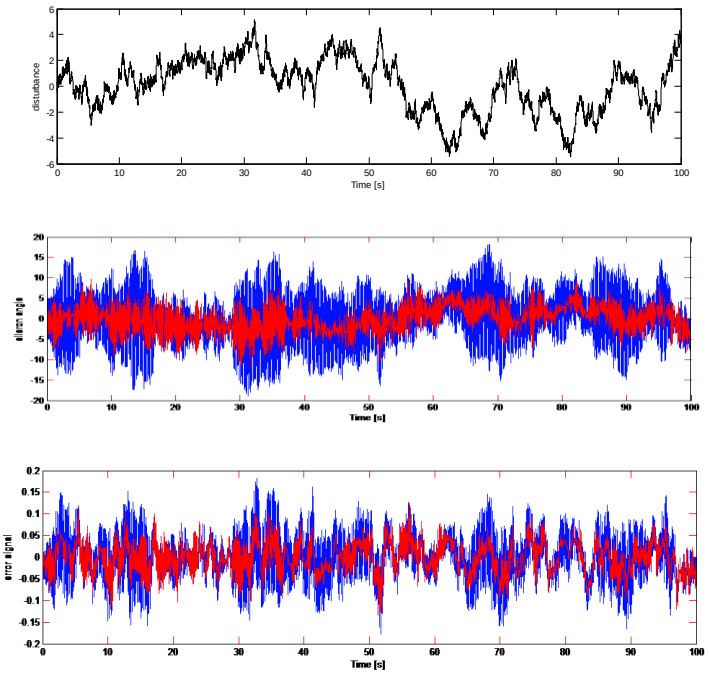

Fig. 9. Behavior of l_1-optimal lateral autopilot without (red color) and with (blue color) unparametric uncertainty

Figs. 8 and 9 show that the behavior of the l_1-optimal autopilot in both situations is satisfactory.

VI. CONCLUSION

This paper dealt with synthesizing and analyzing the digital autopilot which is able to maintain a given roll orientation of an aircraft with a desired accuracy and to cope with an arbitrary external disturbance (a gust). The digital autopilot synthesized as the l_1-optimal controller containing the discrete-time PI and P controller parts.

It was established that the l_1-optimal lateral autopilot may be robust in the presence both of parametric and of nonparametric uncertainties.A distinguishing feature of the control algorithms is that they are sufficiently simple. This is important from the practical point of view.

REFERENCES

[1] D. McRuer, I. Ashkenas, and D. Graham, *Aircraft Dynamics and Automatic Control*, Princeton: Princeton University Press, 1990.

[2] B.L. Stevens and F.L. Lewis, *Aircraft Control and Simulation*, 2nd ed., New York: John Willey & Sons, 2003.

[3] D.E. William, B. Friedland, and A.N. Madiwale, "Modern conrtol theory for design of autopilots for bank-to-turn missiles," *J. Guidance Control*, vol. 10, pp. 378–386, 1987.

[4] E.K. Teoh, D.P. Mital, and K.S. Ang, "A BTT CLOS autopilot design," *The EEE Journal*, vol. 4, pp. 1–7, 1992.

[5] K.S. Ang, *Development of a Flight Control System Using Modern Control Techniques*, M. Eng. Thesis, School of Electrical and Electronics Engineering, Nanyang Technological University, Singapore, 1993.

[6] K.S. Ang, E.K. Teoh, and D.P. Mital, "Adaptive control of a missile autopilot system," in *Proc. 12th IFAC World Congress*, vol. 1, pp. 293–296, 1993.

[7] S.M.B. Malaek, H. Izadi, and M. Pakmehr, "Intelligent autolanding controller based on neural networks," in *Proc. 1st African Control Conference (AFCON2003)*, Cape Town, South Africa, vol. 1, pp. 113–119, 2003.

[8] M.R. Khrosravani, "Apllication of neural network on flight control," *Int. Journal of Machine Learning and Computing*, vol. 6, pp. 882–885, 2012.

[9] E. Lavretsky and K. A. Wise, *Robust and Adaptive Control with Aerospace Application*. London: Springer-Verlag, 2013.

[10] S.R.B. Santos, S.N.G. Junior, C.L.N. Junior, A. Bittar, and N.M.F. Oliveira, "Modeling of hardware-in-the-loop simulator for UAV autopilot controllers," in *Proc. 21st Brazilian Congress of Mechanical Engineering*, Oct. 24-28, Natal, RN, Brazil, 2011.

[11] K.J. Astrom and B. Wittenmark, *Computer Controlled Systems. Theory and Design*, 2nd ed., N.J.: Prentice Hall, Englewood Cliffs, 1990.

[12] G.C. Goodwin, S.F. Graebe, and M.E. Salgado, *Control Systems Design*, N.J.: Prentice Hall, 2001.

[13] J.I. Yuz and G.C. Goodwin, "On sampled data models for nonlinear systems," *IEEE Trans. on Autom. Control*, vol. 50, pp. 1477–1489, 2005.

[14] J.I. Yuz and G.C. Goodwin, *Sampled-Data Models for Linear and Nonlinear System*, London: Springer-Verlag, 2014.

[15] M.A. Dahleh and J.B. Pearson, "l_1-optimal feedback controllers for discrete-time systems," in *Proc. American Control Conference*, Seattle, WA, pp. 1964–1968, 1986.

[16] M. Vidyasagar, "Optimal rejection of persistent bounded disturbances," *IEEE Trans. on Autom. Control*, vol. 31, pp. 527–534, 1986.

[17] M.H. Khammash, "A new approach to the solution of the l_1 control problem: the scaled-Q method," *IEEE Trans. on Autom. Control*, vol. 45, pp. 180–187, 2000.

[18] K.V. Melnyk, L.S. Zhiteckii, A.M. Bogatyrov, and A.Yu. Pilchevsky, "Digital control of lateral autopilot system applied to an UAV: optimal control strategy," in *Proc. 2013 2nd IEEE Int. Conf. "Actual Problems of Unmanned Air Vehicles Developments,"* Oct., 15–17, Kiev, Ukraine, pp. 189–192, 2013.

[19] J.H. Blakelock, *Automatic Control of Aircraft and Missiles*, 2nd ed., New York: John Wiley & Sons, Inc., 1991.

[20] B.T. Polyak and P.S. Shcherbakov, *Robust Stability and Control*, Moscow: Nauka, 2002 (in Russian).

[21] J. T. Tou, *Digital and Sampled-Data Control Systems*, New York: McGraw-Hill Book Company, 1959.

[22] E.I. Jury, *Sampled-Data Conrol Systems*, New York: John Willey & Sons Inc., 1958.

[23] B.T. Polyak, *Introduction to Optimization*, New York: Optimization Softwre Inc., 19

[24] 87.